Effects of inland excess water on bulk density and clay mineralogy of a chernozem soil using xrct and xrpd techniques

Article · January 2017

CITATION
1

READS
78

5 authors, including:

Nuria Gal
Universidad Miguel Hernández de Elche
8 PUBLICATIONS **10** CITATIONS
SEE PROFILE

Tivadar M. Tóth
University of Szeged
115 PUBLICATIONS **515** CITATIONS
SEE PROFILE

Béla Raucsik
University of Szeged
64 PUBLICATIONS **398** CITATIONS
SEE PROFILE

Tamás Földes
TOMOGEO Ltd and GeosoFT Plc
51 PUBLICATIONS **73** CITATIONS
SEE PROFILE

Carpathian Journal of Earth and Environmental Sciences, February 2017, Vol. 12, No. 1, p. 189 - 196

EFFECTS OF INLAND EXCESS WATER ON BULK DENSITY AND CLAY MINERALOGY OF A CHERNOZEM SOIL USING XRCT AND XRPD TECHNIQUES

Norbert GÁL[1], Tivadar M. TÓTH[2], Béla RAUCSIK[2], Tamás FÖLDES[3], & Andrea FARSANG[1]

[1]Department of Physical Geography and Geoinformatics, University of Szeged, Egyetem Street 2–6, Szeged 6722 Hungary, galnorbert@geo.u-szeged.hu;
[2]Department of Mineralogy, Geochemistry and Petrology, University of Szeged, Egyetem Street 2–6, Szeged 6722 Hungary;
[3]Institute of Diagnostic Imaging and Radiation Oncology, Kaposvár University, Guba S. Street 40, Kaposvár 7400 Hungary

Abstract: Inland excess water (IEW) is surplus water in the soil, resulting in long lasting (2–3 months) inundation of areas. The aim of this study is to establish a method to detect differences amongst undisturbed soil cores collected in inundated and non-inundated study plots, in order to reveal the potential effects of IEW on bulk density. In the same patch of Chernozem, two intact soil cores (height 28–32 cm, diameter 19 cm) were sampled in PVC cylinders in an inundated area and, as the control, two more in a non-inundated area. X-ray computed tomography (XRCT) measurements were carried out at a spatial resolution of 660 × 660 μm^2. Higher bulk density, compaction, calculated from the Hounsfield units were recorded by XRCT in the case of the inundated soil columns. As a potential reason for the more remarkable shrinkage observed in the samples affected by inland excess water, the mineralogical composition was analysed by X-ray powder diffraction (XRPD). The measurement confirms the higher proportion of expandable clay mineral phase in the inundated samples compared to the control. Experiments revealed that due to water inundation, secondary clay mineral formation and translocation occurred in the upper horizon of the soil samples, and they can trigger unfavourable structures that enhance the risk of IEW formation.

Keywords: clay minerals, inundation, soil structure, swelling/shrinkage, X-ray computed tomography, X-ray powder diffraction analysis

1. INTRODUCTION

Inland excess water (IEW) is surplus water in the soil, rendering the upper soil saturated on the one hand, and resulting in long lasting (2–3 months) inundation of areas with no runoff on the other (Kozák, 2005). Several hundred thousand hectares of cultivated land in the Pannonian basin are threatened by inundation in early spring periods on account of their hydro-geographical situation (Barta et al., 2016; Kuti et al., 2006). Not only financial (*i.e.* shortfall of crops, the collapse of soaked buildings) but also ecological damage occurs, considering that prolonged water inundation restrains the soil functions (Gál & Farsang, 2013; Miodrag et al., 2013; Pálfai, 2000).

Despite numerous studies, there are no concordant stand-points as to the way in which saturation of soil with water modifies the soil structure – does moistening engender compaction of the soil particles or quite the contrary? A decrease in the average soil bulk density was measured by Pires et al., (2005) after submitting the samples to wetting and drying cycles. Rajaram & Erbach (1999) reported that a single wetting–drying cycle may change the clay–loam soil properties, resulting in an increase in cone penetration resistance, soil cohesion, adhesion and aggregate size. According to Rasa et al., (2012), fine clay intrusions can be attributed to clay dispersion during the spring thaw or prolonged water inundation, resulting in compaction of the soil structure.

The structural behaviour of soil towards water content variations depends on the clay mineralogy, amongst other factors (*e.g.* organic matter content). Since clay minerals are very sensitive to environmental changes, their composition reflects the differences in the soil-forming conditions (Drewnik et

al., 2014). Clay minerals are not only frequently used as indicators of pedogenesis, but clay minerals are also forming from the most recent processes (Bonifacio et al., 2009). For characterising the mineralogical composition of clay fraction in soils, X-ray powder diffraction (XRPD) analysis provides a suitable technique (Drewnik et al., 2014).

X-ray computed tomography (XRCT) provides excellent opportunities to examine the physical behaviour of soil in order to characterize compaction, surface soil sealing and the effects of alterations in water content on soil structure (Crestana & Vaz, 1998; Pires et al., 2010). The technique allows repeated analyses of alterations in the same sample, which cannot be achieved by other classical techniques (Pires et al., 2010). Despite numerous studies (*e.g.* Peth et al., 2010; Pires et al., 2005; Sander et al., 2008), there are few reports about the effects of temporary water inundation on the structure of undisturbed soil samples collected in a larger volume. Considering the presented information, our objective was to reveal the potential effects of inland excess water on soil structure by 1) establishing a method to derive quantitative data from XRCT, in order to analyse the change of bulk density of undisturbed soil cores collected in a frequently inundated study area, and 2) relating the results obtained by XRCT with clay mineral composition of the samples, analysed with XRPD.

2. MATERIALS AND METHODS

2.1. Sample collection and soil analysis

The study area is located on arable land in Békés County, in the Southern Hungarian Great Plain. The area is characterized by extremely low relief, therefore local depressions of the study area have no run-off, and in the spring thaw or in the event of heavy rainfall, ponds and patches frequently form with temporary water inundation. To compare periodically inundated with non-inundated areas, we used Landsat TM images to define borderlines for the most intense advances of the IEW inundation in the past decade (for April 2000, June 2006 and July 2010). As a result, territories inundated every year involved in the analysis and territories without water inundation were delineated.

We collected two intact topsoil core samples (SI-1 and SI-2, "soil inundated") in the former inundated territory (46°18'46"N, 20°45'42"E) and two other soil cores as control (SC-1 and SC-2, "soil control"; 46°18'47"N, 20°45'46"E).

Intact soil cores were sampled in PVC cylinders with an inner diameter of 190 mm. The heights of samples SI-1 and SI-2 were 28.5 and 28.2 cm, and the heights of the control samples (SC-1 and SC-2) were 31.9 and 32.2 cm.

At the proximate location of inundated and control sample points, disturbed soil samples were also taken at 20-cm intervals vertically from two 150-cm-deep boreholes, in order to analyse the basic soil properties. The pH (H_2O, soil:solution ratio 1:2.5) was recorded using a digital pH meter (type WTW Inolab pH 720). The carbonate content of the dry soil samples as a percentage was determined via Scheibler type calcimetry. The total salt content was measured by recording the electric conductivity of the fully saturated soil samples by applying a conductivity meter (type Thermo Scientific Orion 3-Star OK-104). Particle density was measured by the pycnometer method. The organic content was measured after H_2SO_4 digestion in the presence of 0.33 M $K_2Cr_2O_7$ using a spectrophotometer, type UNICAM Helios Gamma UV-VIS. Particle size distribution was measured using Fritsch Analysette 22 laser equipment with a measurement range of 0.08–2000 μm.

2.2. Scanning and image analysis

Intact soil cores were scanned with a medical X-ray CT scanner (Siemens Somatom Sensation Cardiac CT scanner, 120 kV, 250 mAs). Samples were scanned two times: first, at initial moisture content (after sampling), and second, after drying (for 3 months at room temperature, then in a drying set-box for 48 hours at a temperature of 60°C). One hundred and sixty slices were taken vertically from a soil core, and saved as DICOM files (512×512 pixels, 16 bit). The slice thickness was 1.2 mm and the spatial resolution of the images was 660 μm × 660 μm for every pixel. In order to avoid the compaction effect caused by the PVC cylinder wall (Pires et al., 2005), 120×120 mm^2 cuboids were aligned to the sample centre along the soil columns with a volume of 120×120×300 mm^3 (for the SI samples) and 120×120×340 mm^3 (for the SC samples). In the case of each cuboid, regions of interest (ROIs) were appointed with an area of 10×120 mm^2 in each 1 cm depth vertically (Fig. 1).

Every voxel of the tomographic slice is characterized by a Hounsfield unit (HU). A strong linear causal relationship exists between the measured HU-values and the porous medium of the soil; consequently, soil physical parameters, such as bulk density, could be derived from the HU values (Rogasik et al., 2003).

Before the evaluation of the HUs of the image voxels, the representative elementary volume (REV) needs to be defined. There were 100 ROIs one behind another at each 1 cm depth. The HU_{mean} values of the

ROIs were averaged by the simple moving average (SMA) method, and the CV of the HU_{mean} values was examined depending on the SMA window length.

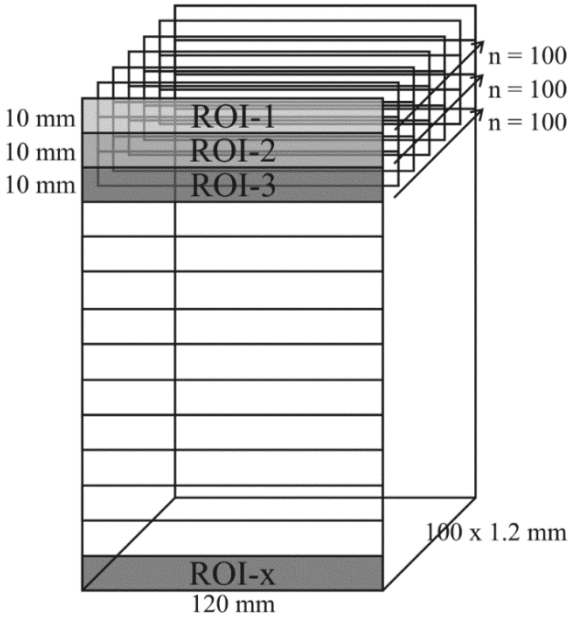

Figure 1. The appointed regions of interest (ROIs) in the intact soil cores

Comparative analyses were carried out between the data of the SI-1, SI-2, SC-1 and SC-2 samples for the actual moisture content at sampling and also after drying. Before evaluation of the measured data, having regard to the few samples, the Shapiro–Wilk test was carried out in order to check the normality of the data. Other than the HU_{mean} data of the SI-1 sample, no samples showed a normal distribution; therefore, the non-parametric related samples Wilcoxon signed rank test was applied for statistical comparison.

In order to derive the soil physical parameters, HU values were calculated into bulk density values using the equations by Rogasik et al., (2003) and Schrader et al., (2007). Image analysis was carried out by Syngo CT 2007S and Osiris 4.19 software and the data were analysed with MS Office and the IBM SPSS Statistics 20 software package.

2.3. X-ray powder diffraction analysis (XRPD)

XRPD analysis was carried out in order to determine the clay mineralogical composition. Powder samples were prepared from three determined depths of the SI-2 and SC-2 soil columns (SI-2: 10–12, 20–22 and 26–28 cm, SC-2: 10–12, 20–22 and 28–30 cm). Aspects of determination of the sampling depths were as follows: 1) one sample represents the zone of the lowest and the other of the highest differences between the bulk density values of the initial (wet) and dried cores; 2) the third subsample represents the plough pan.

The clay fraction was tested for clay mineral determination on oriented specimens deposited on glass slides. Oriented samples were prepared for air-dried and ethylene-glycol solvated testing, and for heat treatment testing at temperatures of 350°C and 550°C. Ethylene-glycol saturation was obtained by vapour immersion of the samples for 8 h at 80°C. XRPD analyses were performed on a Rigaku Ultima IV diffractometer (Cu-Kα1, Bragg-Brentano geometry, secondary graphite monochromator). Bulk-soil disoriented samples were measured using a 3–70°2θ diffraction angle range, step-scan 0.05°2θ and a 3 s/step counting time. Oriented clay fraction samples were measured in the range of 3–50°2Θ with 0.1°2θ steps and a 6 s/step counting time. Semi-quantitative compositions of the bulk samples were determined by the reference intensity ratio method. The semi-quantitative composition of the clay fraction was calculated by the integrated area of the conventionally used basal reflections and correction factors of Rischák & Viczián (1974).

3. RESULTS

3.1. Basic soil properties

Considering the soil properties, the soil was classified as a Calcic Chernozem (Loamic, Pachic) according to the World Reference Base of Soil Resources (2006). In the SC borehole, the soil parameters (*e.g.* pH, total salt content, carbonate content) change gradually following a trend, while the ones in the SI inundated borehole show a greater vertical differentiation and translocation (Fig. 2). This is confirmed by the accumulation of silt and clay fraction below the depth of 80 cm and by the translocation of carbonate into a deeper zone.

In the case of the intact soil core affected by IEW, the reductions in volume were 11.1% on average and in the case of the control columns 5.9%. A remarkable difference in moisture content was determined between the inundated and control soil columns; in the case of the SI cores 34.7–37.9 V/V% and in the SC columns 26.3–27.2 V/V% in the initial wet state (Table 1).

3.2. XRCT-aided soil structure analysis

3.2.1. Representative elementary volume (REV)

The REV was estimated by the value on the x-axis (SMA window length) at a threshold, where the graph of the function was nearly asymptotic (Fig. 3). This was accepted by an SMA window length of 60

(number of integrated slices = 60) and a mean CV value of nearly 0.02. A volume of 60 ROIs (60x1440mm^3=86400mm^3) was calculated as the REV. Hence, further investigations were conducted with derivation of HU values from the 86.4 cm^3 REV at every 1 cm depth in the soil columns.

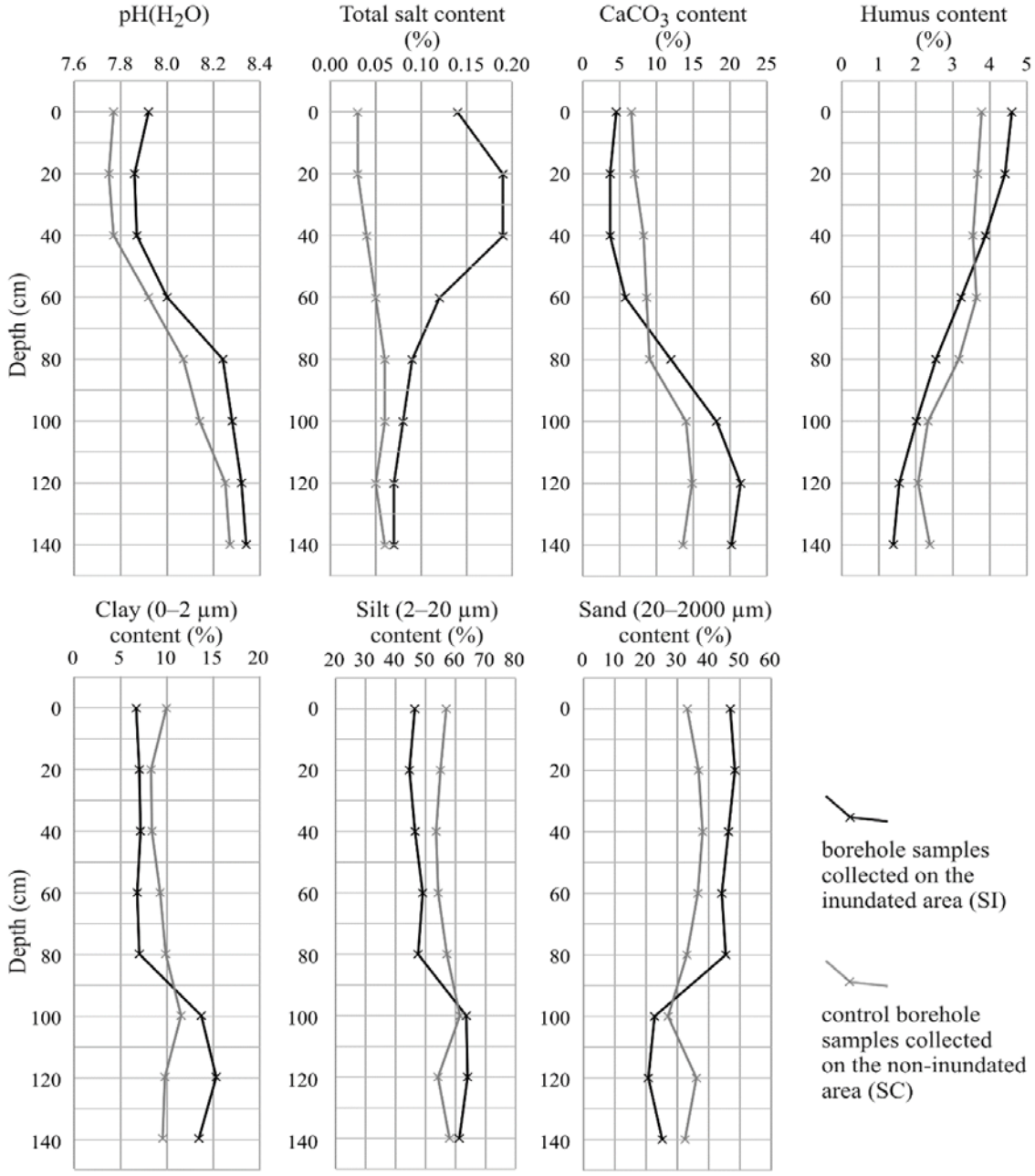

Figure 2. Vertical change of basic soil properties along the boreholes

Table 1. Basic soil properties of intact soil cores determined by volume- and mass-measuring methods (calculated for the total volume of the sampled soil columns)

Sample	Moisturecondition	Average height (cm)	Volume (cm^3)	Bulk density (g/cm^3)	Moisture content (V/V%)
SI-1	After sampling, in wet condition	28.5	8 080.57	1.40	34.7
SI-2		28.2	7 995.51	1.48	37.9
SC-1		31.9	9 044.57	1.48	26.3
SC-2		32.2	9 129.62	1.44	27.2
SI-1	After drying, in dry condition	25.4	7 201.63	1.57	–
SI-2		25.0	7 088.22	1.68	–
SC-1		30.2	8 562.57	1.56	–
SC-2		30.1	8 534.21	1.55	–

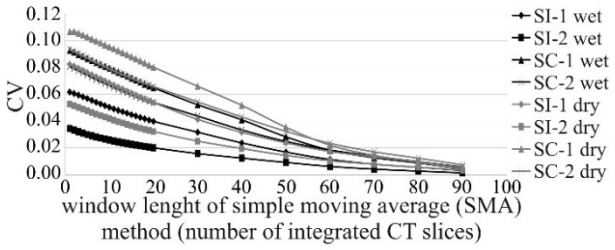

Figure 3. Function between the variation of mean CV values in SI and SC cores and the window length of the SMA method (number of integrated CT slices); the threshold was defined at an SMA window length of 60 integrated slices where 60 ROIs one behind another were integrated at each cm depth in the whole soil column

3.2.2. Comparative analysis between inundated and control soil core samples

Tests verified significant ($p<0.05$) differences between the SI and SC samples. In soil cores affected by IEW, the BD_{mean} values were 1.44 and 1.51 g/cm^3 in the initial condition, and 1.62 and 1.71 g/cm^3 after drying. In the control soil cores, 1.45 and 1.48; and 1.54 and 1.59 g/cm^3 values, respectively, were measured.

The structural pattern of the upper 30 cm of the soil profile can be well represented through the variation in BD values along the soil columns (Fig. 4). Lower BD values down to the depth of 5-7 cm show loose, unconsolidated soil aggregates, where values between 5-7 and 25-27 cm indicate the relatively homogeneous cultivated horizon, while the increase in BD values under the depth of 25-27 cm may relate to the more compact plough pan.

In the case of the inundated soil columns, differences between the BD values in the wet and dry condition are greater (with an average of 0.18 and 0.20 g/cm^3 values in SI-1 and SI-2) than those recorded in the case of the control samples (0.08 and 0.11 g/cm^3 in SC-1 and SC-2).

In the case of the samples affected by IEW, the mean CV_{BD} values are 0.018 (SI-1) and 0.029 (SI-2); and 0.026 and 0.046 in wet as well as in dry conditions, respectively. The same parameters in the control samples are 0.017 and 0.026 in the wet conditions and 0.058 and 0.030 in the dry. In the case of each sample, slight increases in the CV_{BD} values are characteristic after drying.

3.3. Mineralogical composition based on XRPD analyses

The bulk samples have a relatively uniform mineralogical composition. The dominant minerals of both the SI and SC bulk samples are quartz (30–60%) and micas±illite (20–40%). Chlorite±vermiculite (5–10%), albite (5–10%) and dolomite (up to 5–10% in the sample SC-2 20–22) remain minor constituents. In the sample SC-2 10–12 the presence of amphibole is proven.

Clay minerals identified in the <2μm fraction include illite±mica, kaolinite, chlorite-like phase and mixed-layer phase with a significant smectitic component. Illite±mica is the prevalent phase in both samples with ~60% (SC-2) and ~40% (SI-2) concentrations. The heat treatments suggest the presence of a mixed-layer chlorite/vermiculite and/or chlorite/smectite. Relative amounts of this phase can be estimated at ~10–20% in the SC-2 samples and at ~20–30% in the SI-2. As far as the physical properties of the soils are concerned, the most important clay minerals are the various expandables. Each of the examined samples comprises a phase expanded after ethylene-glycol solvation. This treatment does not produce a sharp ~17 Å basal peak, as is typical of smectite, but a very diffuse reflection in the 15–17 Å range resulted in an emerged baseline. On the other hand, the heating at 350 and 550 °C intensified the 10 Å peak clearly, proving the presence of the smectitic component. The above mentioned properties of the swelling phase suggest that the investigated soils possibly contain a relatively low amount of highly expandable mixed-layer chlorite/smectite and/or illite/smectite. The two examined soil types could comprise this swelling mixed-layer clay mineral in concentrations up to ~20% (SI-2) and up to ~10% (SC-2) (Fig. 5).

4. DISCUSSION

4.1. Structural differences between SI and SC core samples

XRCT proved to be a better method than other traditional methods such as collecting small undisturbed soil cores, considering that application of XRCT enables 1) repeated investigations of undisturbed samples in a larger volume, 2) selection of different regions of interest in the same sample, 3) visualization of the inside of the sample, and 4) exclusion of disturbing effects (*e.g.* compaction effect at the wall) in the sample.

In this investigation, a volume of ~86.4cm^3 was accepted as representative. This volume coincides well with the results of former research, such as that of Borges & Pires (2012), who revealed that samples with volumes from 50 to 100 cm^3 with a minimum cross-section of 6.4 cm^2 are large enough to characterize soils with bulk density values. A 3% variation among BD values derived from HUs and measured by the volume- and mass- measuring method was observed, which coincides with the variation measured by Pedrotti et al., (2005) in their study.

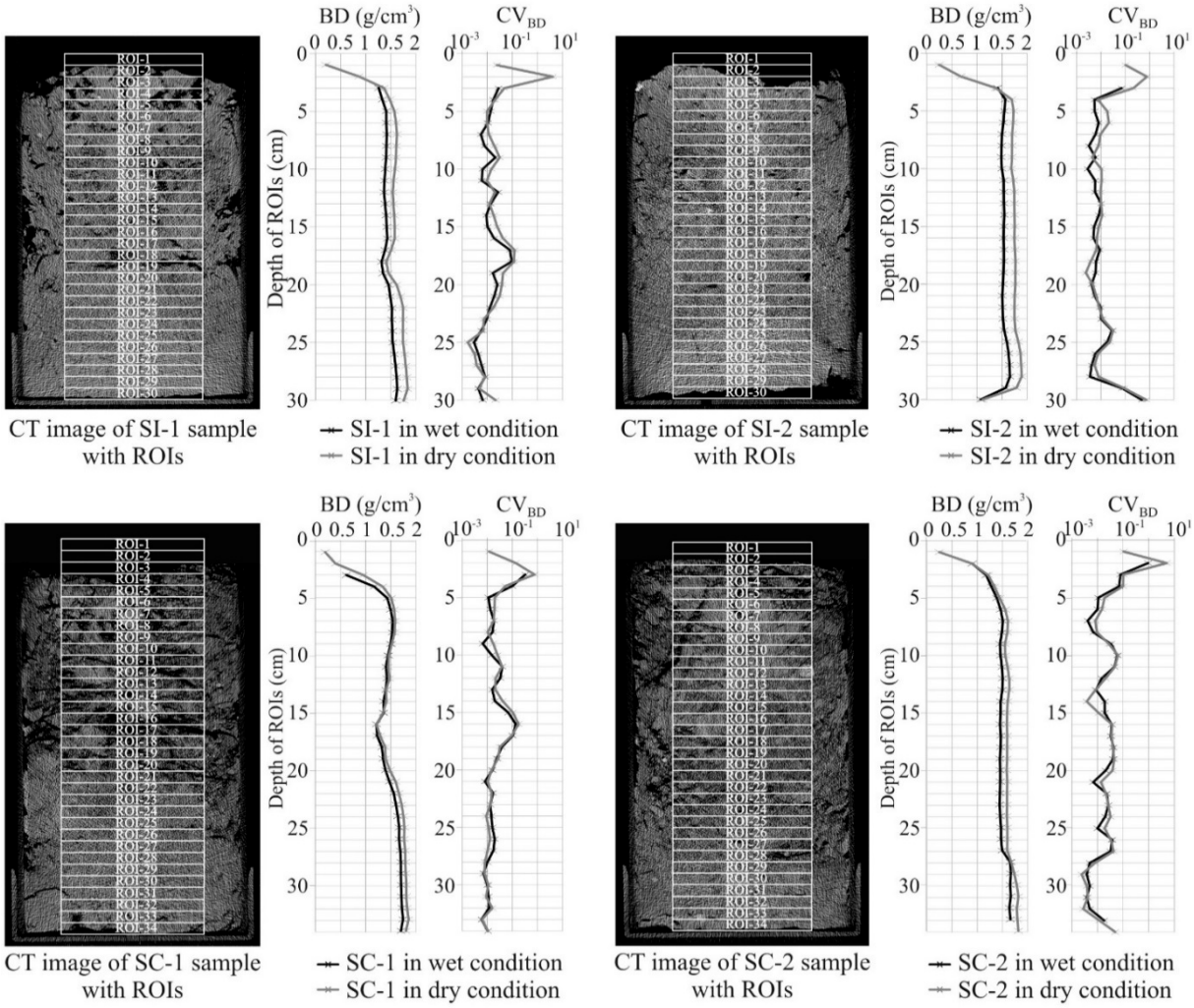

Figure 4. Vertical profiles of bulk density (BD) and coefficient of variation of bulk density (CV_{BD}) values in the inundated (SI-1 and SI-2) and control (SC-1 and SC-2) intact soil cores in wet and dry condition. Each value in the vertical profiles is calculated with regard to the representative elementary volume (REV) derived at every 1 cm depth in the soil columns

After the samples were dried, the total volume decreased and the dry BD values increased in both the SI and SC samples, showing evidence of shrinkage. A more notable increase of BD values was observed in the SI cores, consequently, a higher compaction was detected in the samples affected by IEW.

Increase in CV_{BD} values was measured after samples were dried, and larger increases were experienced in the SC samples (especially in SC-1). According to the lower variation values of SI samples, the macro-structure of the inundated samples showed less heterogeneity than that of the control samples. This might be explained by the denser and more compacted structure of the dried SI samples as the result of the potential effect of IEW inundation. The more homogeneous structure suggests disaggregation in the inundated samples, which was also observed by Rajaram & Erbach (1999), after submitting their samples to a wetting and drying cycle.

4.2. Clay minerals

XRPD analysis revealed that the SI-2 and SC-2 samples differed not only in their structural properties but also in their mineralogical composition. The qualitative and semi-quantitative analysis revealed that the chlorite±vermiculite and mixed-layer phase contents of the SI-2 samples were 10% higher, while the micas±illite phase content was 20% lower than those of the SC-2 samples. Physical soil properties and reversible swelling and shrinkage processes are strongly influenced by expandable phase (Stern et al., 1991). Although vertical differences in the mineralogical components cannot be observed in the soil columns, it can be declared that there is higher content of expandable phase in the SI-2 to SC-2 samples, which can explain the more significant shrinkage of the SI-2 samples due to drying.

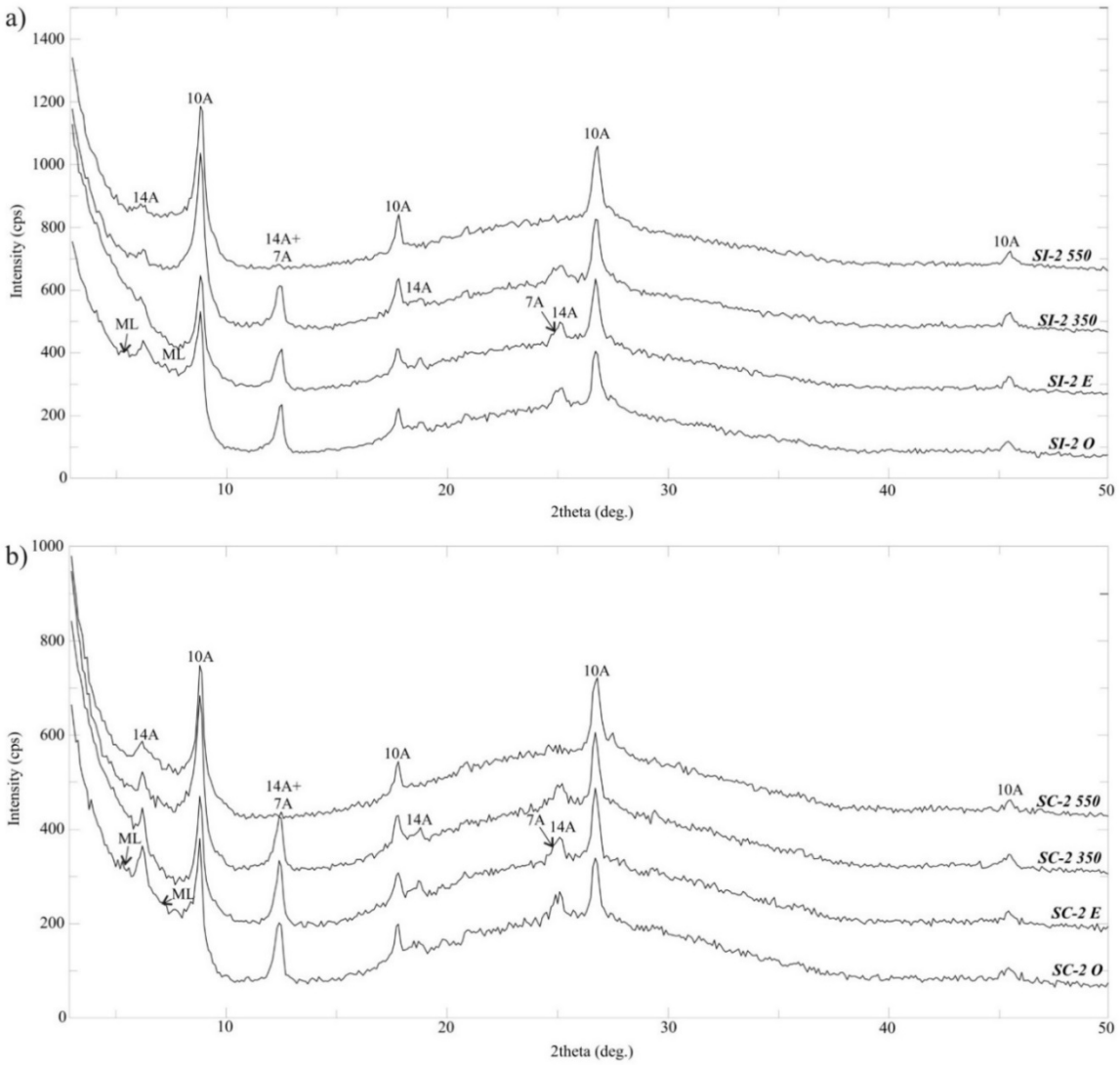

Figure 5. Typical X-ray powder diffraction pattern of oriented specimens of the **a)** SI-2 soil represented by the SI-2 20-22 sample, and **b)** SC-2 soil represented by the SC-2 20-22 sample, based on air-dried (O), ethylene-glycol saturated (E) and heat-treated (350°C and 550°C) measurements. Abbreviations: ML: mixed-layer phase; 14A: 14 Ångström phase; 10A: 10 Ångström phase; 7A: 7 Ångström phase

Since differences in the vertical distribution of the mineralogical composition of the soil columns were not observable, instead of translocation, secondary formation of clay minerals is assumed to be the reason for the higher expandable phase in the samples of the SI cores compared to the SC cores. Consequently, besides leaching, disaggregation, and compaction, water inundation also influenced the clay mineralogy by initiating secondary clay mineral formation.

5. CONCLUSIONS

In this paper, XRCT and XRPD techniques were applied, in order to investigate the potential effects of temporal water inundation, caused by IEW, on soil structure and clay mineralogy.

– Leaching was observed in the translocation of clay and silt fraction and the accumulation of $CaCO_3$ at the bottom of the soil profile.
– Higher bulk density and compaction were observed in the soil columns collected from the inundated area. More notable shrinkage of inundated samples was experienced after drying of the soil cores; consequently, differences between the mineralogical compositions of the inundated and control samples were assumed.
– Mineralogical components were analysed using the XRPD technique, which proved the higher expandable phase of the inundated samples compared to the control. Expandable phase consisted mainly of illite/smectite and chlorite/smectite mixed-layer phases.

Experiments revealed that due to water inundation, secondary clay mineral formation and translocation occurred in the upper horizon of the soil samples,

which can trigger unfavourable structures that enhance the risk of IEW formation.

Acknowledgements

This research was supported by the European Union and the State of Hungary, co-financed by the European Social Fund in the framework of TÁMOP 4.2.4.A/2-11-1-2012-0001 'National Excellence Program'.

REFERENCES

Barta, K., Szatmári, J. & Posta, Á., 2016. *Connection between inland excess water development and motorways.* Carpathian Journal of Earth and Environmental Sciences, 11, 1, 293–301.

Bonifacio, E., Falsone, G., Simonov, G., Sokolova, T. & Tolpeshta, I., 2009. *Pedogenic processes and clay transformations in bisequal soils of the Southern Taiga zone.* Geoderma, 149, 66–75.

Borges, J.A.R. & Pires L.F., 2012. *Representative elementary area (REA) in soil bulk density measurements through gamma ray computed tomography.* Soil & Tillage Research, 123, 43-49.

Crestana, S. & Vaz, C.M.P., 1998. *Non-invasive instrumentation opportunities for characterising soil porous system.* Soil & Tillage Research, 47, 19–26.

Drewnik, M., Skiba, M., Szymański, W. & Żyła, M., 2014. *Mineral composition vs. soil forming processes n loess soils – A case study from Kraków (Southern Poland).* Catena, 119, 166–173.

Gál, N. & Farsang, A., 2013. *Weather extremities and soil processes: Impact of excess water on soil structure in the South Hungarian Great Plain.* In: Lóczy D. (Ed.), Geomorphological Impacts of Extreme Weather: Case Studies from Central and Eastern Europe. Springer Geography, Springer, Heidelberg, 313–325.

IUSS Working Group WRB, World reference base for soil resources 2006, 2006. *World Soil Resources Report No. 103.* FAO, Rome

Kozák, P., 2005. *Inland excess water regime on the SE Hungarian Great Plain in context of the European water management requirements.* PhD thesis, University of Szeged, Faculty of Science and Informatics, Szeged (in Hungarian)

Kuti, L., Kerék, B. & Vatai, J., 2006. *Problem and prognosis of excess water inundation based on agrogeological factors.* Carpathian Journal of Earth and Environmental Sciences, 1, 1, 5–18.

Miodrag, B., Obradovic, D., Dudarin, Z., Barta K. & Zivanov M., 2013. *Measurement and monitoring system for level of groundwater.* Key Engineering Materials, 543, 243–246.

Pálfai, I., 2000. *Excess water risk and drought sensitivity of the Hungarian Plain.* In: Pálfai I. (Ed.), The role and importance of water on the Hungarian Great Plain), Nagyalföld Alapítvány Vol 6, Békéscsaba, 85–95. (in Hungarian)

Pedrotti, A., Pauletto, E.A., Crestana S., Holanda F.S.R., Cruvinel P.E. & Vaz C.M.P., 2005. *Evaulation of bulk density of Albaqualf soil under different tillage systems using the volumetric ring and computerized tomography methods.* Soil & Tillage Research, 80, 115–123.

Peth, S., Nellesen, J., Fischer. G. & Horn, R., 2010. *Non-invasive 3D analysis of local soil deformation under mechanical and hydraulic stresses by μCT and digital image correlation.* Soil & Tillage Research, 111, 3–18.

Pires, L.F., Bacchi, O.O.S. & Reichardt, K., 2005. *Gamma ray computed tomography to evaluate wetting/drying soil structure changes.* Nuclear Instruments and Methods in Physics Research, 229, 443–456.

Pires, L.F., Borges, J.A.R., Bacchi, O.O.S. & Reichardt, K., 2010. *Twenty-five years of computed tomography in soil physics: A literature review of the Brazilian contribution.* Soil & Tillage Research, 110, 197–210.

Rajaram, G. & Erbach, D.C., 1999. *Effect of wetting and drying on soil physical properties.* Journal of Terramechanics, 36, 39–49.

Rasa, K., Eickhorst, T., Tippkötter, R. & Yli-Halla, M., 2012. *Structure and pore system in differently managed clayey surface soil as described by micromorphology and image analysis.* Geoderma, 173-174, 10–18.

Rischák G. & Viczián I., 1974. *Mineralogical factors determining the intensity of basal reflections of clay minerals.* MÁFI Évi Jelentés 1972-ről, 229–256.

Rogasik, H., Onasch, I., Brunotte, J., Jégou, D. & Wendroth, O., 2003. *Assessment of soil structure using X-ray tomography.* In: Mees F., Swennen R., van Geet M., Jacobs P. (Eds.), Applications of X-ray Computed Tomography in Geosciences. Geological Society, London, Special Publications, 215, 151–165.

Sander, T., Gerke, H.H. & Rogasik, H., 2008. *Assessment of Chinese paddy-soil structure using X-ray computed tomography.* Geoderma, 145, 303–314.

Schrader, S., Rogasik, H., Onasch, I. & Jégou, D., 2007. *Assessment of soil structural differentiation around earthworm burrows by means of X-ray computed tomography and scanning electron microscopy.* Geoderma, 137, 378–387.

Stern, R., Ben–Hur, M. & Shainberg, I., 1991. *Clay mineralogy effect on rain infiltration, seal formation and soil losses.* Journal of Soil Science, 152, 455–462.

Received at: 09. 03. 2016
Revised at: 14. 10. 2016
Accepted for publication at: 31. 11. 2017
Published online at: 10. 11. 206